Visual Abstract

Investigation fatigue crack initiation and propagation cruciform welded joints by extended finite element method (XFEM) and implementation SED approach

Djeloud Hamza, Moussaoui Mustafa
Laboratory of Development in Mechanics and Materials (LDMM) - University of Djelfa, (17000) Algeria.
hamzadjaloud@gmail.com, http://orcid.org/0000-0002-0726-3466
moussaoui_must@yahoo.fr

Kellai Ahmed
Research Center in Industrial Technologies, CRTI, P.O. Box 64, Cheraga, 16014 Algiers, Algeria.
a.kellai@crti.dz

Hachi Dahmane
Laboratory of Development in Mechanics and Materials (LDMM) - University of Djelfa, (17000) Algeria.
hachi_dahmane@yahoo.fr

Filippo Berto
Department of Mechanical and Industrial Engineering, NTNU – Norwegian University of Science and Technology, Trondheim, Norway.
filippo.berto@ntnu.no, http://orcid.org/0000-0002-4207-0109

Benattou Bouchouicha
Laboratory of Materials and Reactive Systems (LMSR), Department of Mechanical Engineering, University of Sidi-Bel-Abbes, Bp 89, cité Ben M'hidisidi- Bel-Abbes 22000-Algeria.
benattou.bouchouicha@gmail.com, https://orcid.org/0000-0002-6051-5108

Hachi Brahim Elkhalil
Laboratory of Development in Mechanics and Materials (LDMM) - University of Djelfa, (17000) Algeria.
br_khalil@yahoo.fr, http://orcid.org/0000-0002-6672-746X

ABSTRACT. This study has used the strain energy density (SED) approach to evaluate the stress intensity factor (SIF) of cracked cruciform welded joints in Hardox 450 steel. A microstructural analysis was made of Hardox 450 steel which is composed of refined and tempered low carbon martensite. The

OPEN ACCESS

Citation: Djeloud, H., Moussaoui, M., Kellai, A., Hachi, D., Berto, F., Bouchouicha, B., Hachi, B. E., Investigation fatigue crack

obtained results of simulation will be compared with those provided by J-integral method for different enriched zones and contours based on the extended finite element method (XFEM) coupled with the level set technique (LST). Crack initiation and propagation under cyclic loading have been adopted for the modeling of cruciform welded joints.

KEYWORDS. Strain energy density approach; XFEM; Stress intensity factor; crack initiation and propagation; Hardox 450.

initiation and propagation cruciform welded joints by extended Finite Element Method (XFEM) and implementation SED approach, Frattura ed Integrità Strutturale, 60 (2022) 346-362.

Received: 13.02.2022
Accepted: 22.02.2022
Online first: 02.03.2022
Published: 01.04.2022

INTRODUCTION

Welding is an efficient and long lasting joining procedure. The various welding types are used in almost all industries. However, the welding operation, usually creates different types of defects, like cracks, porosity, elemental segregation, and brittle phases. These defects significantly decrease the fatigue life [1,2]. XFEM has been successfully applied to solve many welding-related problems. For instance, Kai uses XFEM to create a repaired welding model of welded joints of P91 steel plates with particular cracks[3]. Chen et al. build a numerical model by XFEM and experimental investigation of crack growth in T-joints to better understand the mechanisms of crack growth in welded joints [4]. Wang et al. also used XFEM for numerical simulation of the fatigue crack growth and suggested developing simple solutions for practical prediction of M_k factors [5]. XFEM will be utilized to make a model of a semi-elliptical weld toe crack in a fillet weld for different sizes. The obtained M_k parameter is represented in the form of curves as a function of crack dimensions. Pang makes use of the volumetric approach to evaluate the SIF in a pipe made P264GH steel under internal pressure by adopting XFEM [6]. He chose P264GH due to its weldability and ductility properties that help make this material appropriate for piping [7]. Taheri used XFEM to evaluate the effects of welding residual stresses on crack growth rate[8]. Kraedegh et al. in [9] examined fatigue crack growth in T joints under three-point bending that were simulated numerically by XFEM. Chatziioannou et al. manufactured X-joint specimens, S420 steel and used them [10]. A comparative study between repaired and unrepaired cruciform welded. A new correlation was proposed to assess the SIF of repaired cruciform welded joints based on the reduction and the correction factors of un-repaired cruciform welded joints [11]. They are vulnerable to high cyclic loading, and rigorous numerical models are used to simulate the experimental Can provide accurate predictions [12–15].

There are various approaches that can be used for assessment of the SIF of welded joints, peak stress, volumetric approach, and average strain energy density[16–18]. We implemented the last one in the XFEM couple with level set technique because it is faster and less resource consuming. In this study, we use a code developed by Hachi and his team that was used to solve problems involving cracks in case of static and dynamic load and crack growth prediction, homogenization in 2D and 3D, etc [19–21].

Sih developed the SED theory for the purpose of solving fracture mechanics problems [22–24]. He identified the global and local strain energy density, as well as the fracture behavior factors. Lazzarin and co-workers were the first to formalize and publish a series of very crucial papers using a synthesis based on the ASED calculated in the control volume are around the crack tip or U-notched or V-notched, See references [25–29]. many researchers utilize the strain energy density criterion investigated experimentally and numerically in case of brittle materials [30][31]. Lazzarin studied ductile materials and in-plane tensile loading mode I. However, mode II is generally negligible in applications[32]. To estimate the NSIFs directly from local stress distributions, we need very fine meshes. Note that refined meshes are not required when the goal of the finite element analysis is to estimate the average value of the local strain energy density on a control volume surrounding the V-notches or crack tip [33]. The SED approach has been successfully used by Aliha et al. in mixed mode (I/II). Aliha also studied sharp notched disc bend specimens under mixed mode (I/III) loading [34][35], Campagnolo et al. characterized different control volumes and exposed them to different combinations of static loading types in order to evaluate the resistance of different materials, [36–38]. Furthermore, In the case of cracks subjected to mixed mode (I/II) loading, the relationship between the averaged strain energy density SED technique and the peak stress method has been explored [39]. Just a few number of studies used SED approach to analyse cruciform welding joint with predefined cracks. That's why we were interested in this study in using this approach in XFEM to evaluate SIF value and compare it with another SIF value

obtained using J-integral. The paper is organized in the following way. Section 2 describes the materials and models used in this study. Section 3 microscopic study of the state for different welding regions weld metal (WM), heat affected zone (HAZ), basse metal (BM) Section 4.1 provides the theoretical background of the ASED approach. In subsection 4.2 we show the theoretical background XFEM, and in subsection 4.3 we present the theory of Level-set technique. Section 5 describes the method adopted to get results in two phases, the first part of static load, and the second part in fatigue load. Section 6 summarizes the main conclusions of the paper.

MATERIALS AND MODELS

High-strength steel is used to make cruciform welded joints made of high-strength martensitic abrasion resistant Hardox 450 steel. Chemical composition of the base metal, weld metal and mechanical properties are indicated in Tab. 1, Tab. 2, and Tab. 3 respectively. All data from Tabs. 1, was determined using a Thermo Fisher Scientific instrument. For the manufacturing of steel structures like steel bridges, offshore structures, etc. Welding is nowadays considered an efficient metal joining process. The type of fillet welded cruciform joint is commonly used in the construction of long spanned bridges with improved design and higher weld quality. However, the existence of geometrical discontinuities such as cracks and porosity in addition to metallurgical nonuniformities, which lead to crack initiations from different positions that can be difficult to detect [40].

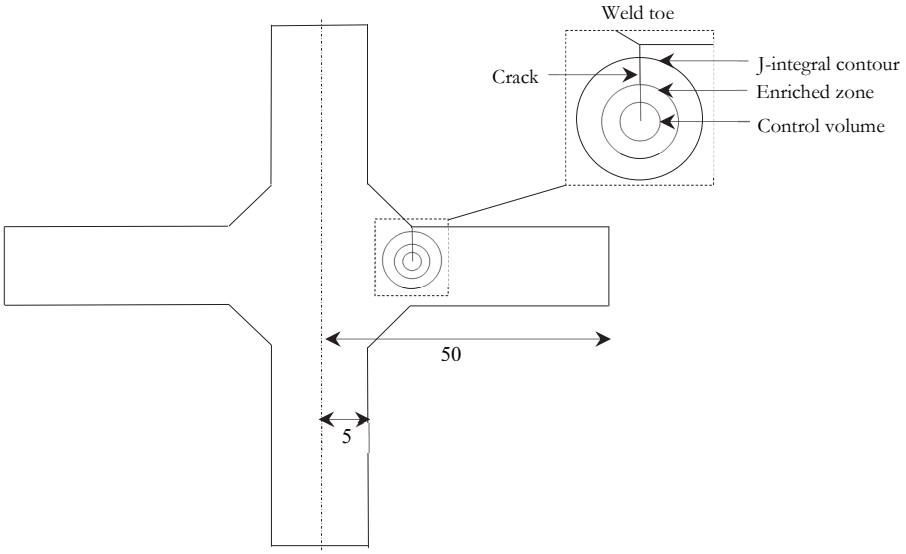

Figure 1: Geometry and dimension of cruciform welded joints involves a cracks specimen (mm scale).

C	Si	Mn	Cr	Ni	Mo
0.21	0.7	1.6	0.25	0.25	0.25

Table 1: Chemical composition Hardox 450.

C	Si	Mn
0.11	0.8	1.5

Table 2: Chemical composition of the electrode.

E(GPa)	σ_t (MPa)	K_{IC} (MPa(mm)$^{0.5}$)	A%	ν
210	1660	3067	7	0.29

Table 3: Mechanical properties of Hardox 450.

NUMERICAL MODELLING

The local strain energy density SED approach is one of such modern methods, currently used in the evaluation of fatigue. The main idea of the SED method is to fully surround the crack tip or notch tip with a size control volume to calculate the strain energy for each finite element that can be achieved through the Eqn. 1.

$$W_i = \frac{1}{2E}\left(\sigma_{xx}^2 + \sigma_{yy}^2 + \sigma_{zz}^2 - 2\nu\left(\sigma_{xx}\sigma_{yy} + \sigma_{xx}\sigma_{zz} + \sigma_{yy}\sigma_{zz}\right)\right) + 2\left(1+\nu\right)\sigma_{xy}^2) \tag{1}$$

where $\sigma_{zz} = 0$ under plane-stress and $\sigma_{zz} = \nu\left(\sigma_{xx} + \sigma_{yy}\right)$ under plane-strain [41]. The total average elastic energy included in the area of control volume according to the SED approach is determined by Eqn. 2.

$$W_e = \frac{\sum_1^i W_i}{\sum_1^i A_i} \tag{2}$$

The next stage in the SED calculation is to determine an ideal control volume radius R_c, which varies depending on the material. There are already different investigations about the control volume radius it can be calculated from the Eqn. 3. Generally for steel $0.2 \le R_c \le 0.4$ [42]. For a sharp V-notch, the critical volume becomes a circular sector of radius R_c centered at the notch tip Fig. 2a.

$$R_c = \frac{\left(1+\nu\right)\left(5-8\nu\right)}{4\pi}\left(\frac{K_{Ic}}{\sigma_t}\right)^2 \tag{3}$$

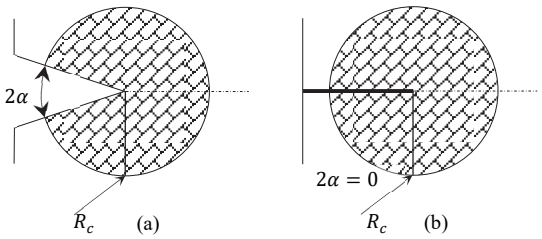

Figure 2: Control volume (a) pointed V-notch (b) crack.

Where ν is the Poisson's ratio K_{Ic} critical stress intensity factor mode I and σ_t conventional ultimate tensile strength. When utilizing the SED approach, it is critical to adjust the finite elements in the control volume to ensure that there are enough finite elements to approximate the actual value[43–45] in the case of using XFEM, the crack tip enrichment and the crack enrichment compensate for the density of the mesh.
The analytical evaluation for the total elastic ASED over the control volume is based on the leading order terms of William's solution and is evaluated as shown in the following equation [33].

$$W_1 = \frac{e_1}{E}\left(\frac{K_I}{R_c^{2(1-\lambda_1)}}\right)^2 \tag{4}$$

E is the Young's modulus which is given for different materials and λ_1 are the eigenvalues of the Williams' stress field solution for the N-SIF K1 for modes I. The eigenvalues λ_1 can be derived from the case of crack λ_1=0.5 [39]. The values for this are already listed in the literature for different important 2α [40]. e_1 correction factors which depend on the stress-

strain field, Poisson's ratio and the notch opening angle 2α. Wither calculation can be made for e_1 from the following empirical equations [46].

$$e_1 = -5.373.10^{-6}(2\alpha)^2 + 6.151.10^{-4}(2\alpha) + 0.133 \tag{5}$$

XFEM coupled to the LST

The displacement field is described by the following finite element approximation equation.

$$u(x) = \sum N_i(x) u_i \tag{6}$$

The XFEM is used to represent the discontinuities independent of the mesh. The discontinuities can be modeled by enriching all discontinuous elements using enrichment functions that satisfy the discontinuous behavior and adding additional nodal degrees of freedom, mention here Belytschko and Moes the first to formalize and publish a series of very important papers using XFEM [47–50].

In general, the approximation of the field of displacement in the XFEM takes the following form.

$$u(x) = \sum_{i \in S} N_i(x) \left[u_i + \underbrace{H(x) a_i}_{n_e} + \underbrace{\sum_{a=1} \varphi_\alpha(x) b_i^a}_{n_f} \right] \tag{7}$$

n_f is the set of nodes are which contains the crack tip (represented by yellow squares on Fig. 3), n_e is the set of nodes entirely cut by the crack (represented by blue circles in Fig. 3). The u_i are the classical degrees of freedom. The a_i are the degrees of freedom linked to the discontinuity and the b_i^a are the degrees of freedom linked to the singularities.

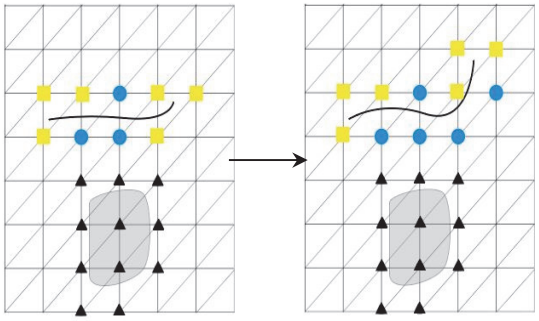

Figure 3: Enrichment strategy in XFEM.

The onset and crack growth are characterized using the Paris law [51], which relates the change in SIF to crack growth rates. The stress intensity factor range can be evaluated by proposed by [52].

$$\Delta K = \sqrt{K_I^2 + K_{II}^2} \tag{8}$$

Once the crack is defined as a level set segment, the model of XFEM evaluate the K_I and K_{II} through this, the increment of the crack is deduced by Eqn. 9.

$$da = C * dN * \left(\frac{\Delta K}{10^6} \right)^m \tag{9}$$

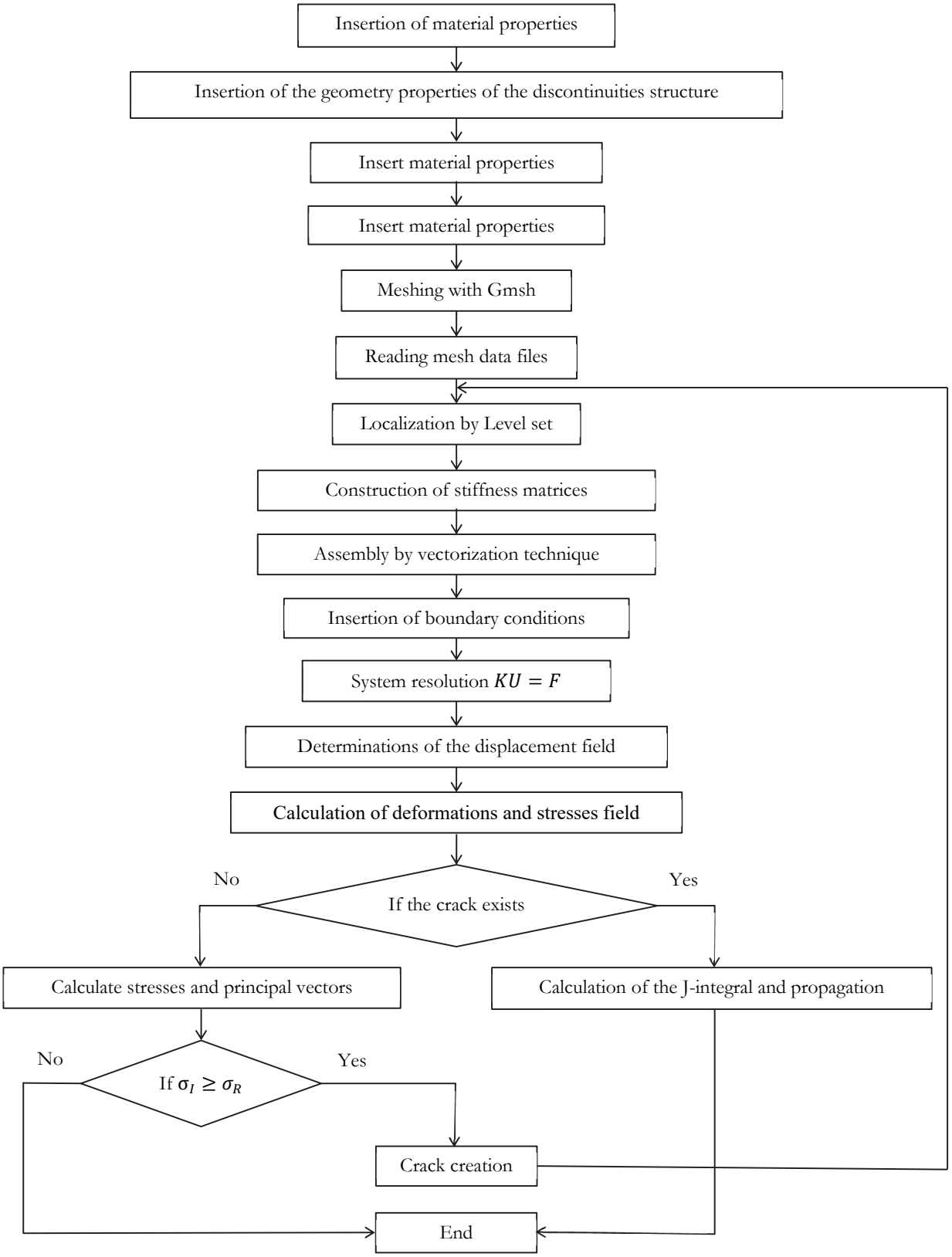

Figure 4: Flowchart of our calculation code.

The maximum circumferential stress criterion is used in this study to determine the direction of the crack growth, which is given by Eqn. 10. The direction of crack growth is a consequence of the mixed-mode stress intensity factors, as can be shown in Eqn. 2, and the crack will propagate in the direction where σ_I is a maximum [53].

$$\vartheta = 2arctangent\left(\frac{1}{4}\left(\frac{K_I}{K_{II}}\right)+\sqrt{\left(\frac{K_I}{K_{II}}\right)^2+8}\right) \tag{10}$$

where K_I and K_{II} are respectively maximum stress intensity factor of mode I and II during cyclic loading.

Level-set technique

The level set method is a numerical technique used for analysing and tracking moving interfaces. The interface can be evolved by representing it with is contours of a level set function ϕ. Without the knowledge of the exact location [54, 55] of the interface, it can be moved implicitly by updating the level set function ϕ. At all times, the interface is represented as its zero level the Eqn. 11 represented the analytical form.

$$\phi(x)=\left(\frac{|x-x_c|}{a_1}\right)^{p_1}+\left(\frac{|y-y_c|}{a_2}\right)^{p_2}-1 \tag{11}$$

Presentation of the developed code

The modeling by XFEM coupled with LST for the evaluation of the basic parameters in fracture mechanics presented in the previous section (Numerical modeling) was programmed according to the flowchart proposed in Fig. 4.

ANALYSIS OF METALLURGICAL TRANSFORMATION

The Hardox 450 steel is characterised by a microstructure of quenching, contains lamellar crystals, which are likely due to γ → α shear transformation, and fragmented α phase crystals with weak misorientations, consist of the martensite with a slate-like morphology with areas of tempered martensite Fig. 5 [56,57].

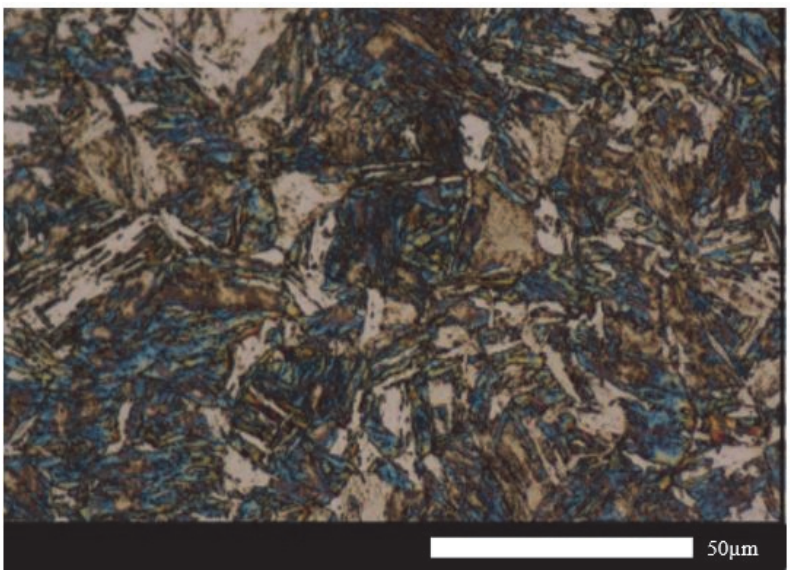

Figure 5: Optical micrograph of base metal BM.

According to the cooling rate and the amount of carbon, the microstructure consists of the refined and tempered low-carbonlath-type martensite with fine acicular ferrite, widmanstatten ferrite and pearlite were formed Fig. 6 [64].

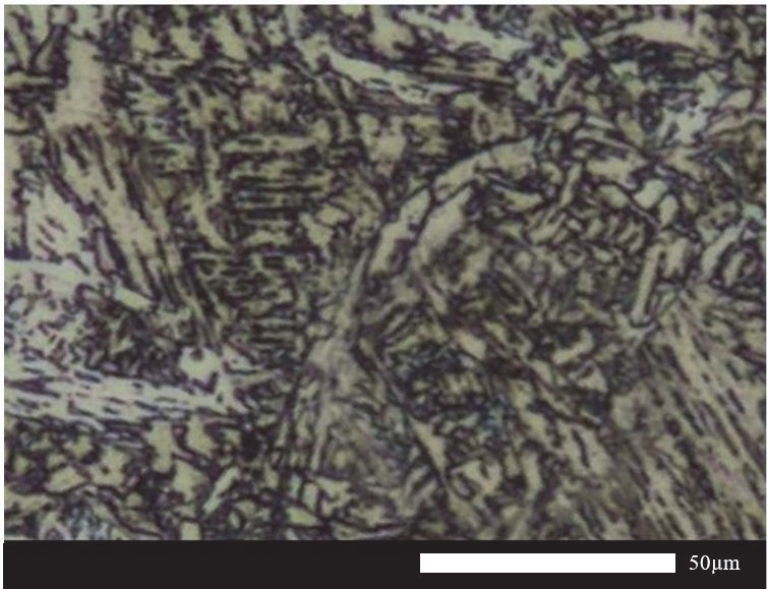

Figure 6: Optical micrograph of heat affected zone HAZ.

The microstructure of the weld metal is dendritic, consists of a fine-grained non-equilibrium (acicular) ferrite, and pearlite structure with troostite precipitates, nucleating mainly at the solidification grain boundaries which results from the lower cooling rate Fig. 7 [58].

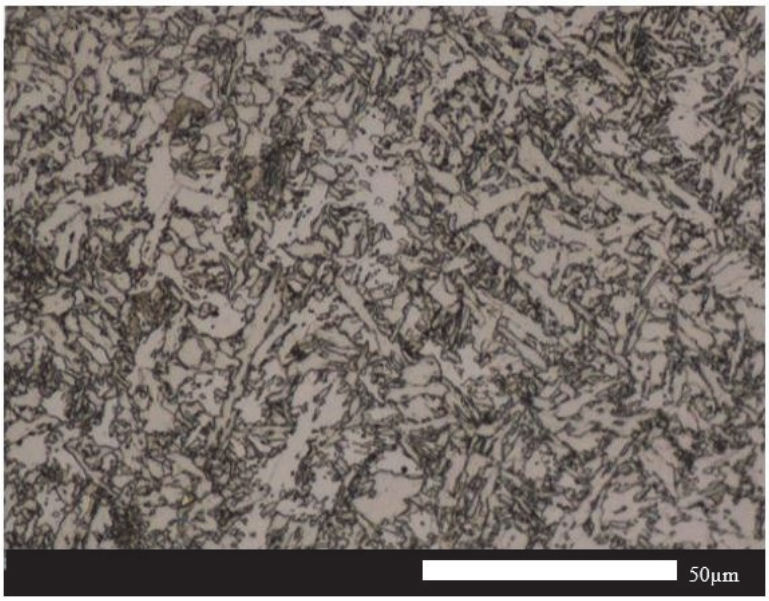

Figure 7: Optical micrograph of weld metal zone WM.

RESULTS AND DISCUSSIONS

After examining a lot of studies, it is clear that few researchers used the SED approach to assess SIF in the case of the cracked component and mention here [59–62]. As stated in the paper F. Berto *'This approach cannot be applied to notch with zero opening angle (cracks) subjected to mixed mode loading'*, this is confirmed in this study, by comparing the results with one of the most effective methods J-integral.

Effect of the static loading

a) Variation in crack length

In this section, cruciform welded joints are made from Hardox 450 modeling by XFEM in 2D plane strain meshing by the triangular element. All the dimensions and boundary conditions are shown in Fig. 1 and Fig. 5. The welding fatigue crack initiation point is difficult to predict accurately because it usually occurs in the vicinity of the weld toe. This has been found in many studies [63,64]. The length of the cracks evolves from 2 mm and increases with step of 1 mm to reach a maximum length of 8 mm. Here, an interest is focused on two study stages: the first stage focuses on the evaluation of the SIF values for several enriched zones of the diameters $3h_e$, $4h_e$ and $5h_e$ (h_e is element size) while keeping the contour of J-integral constant with a diameter equal to $4h_e$, and in the second step keeping the enriched zone constant with a diameter equal to $4h_e$ and the variation will be carried on the diameter of J-integral contours with the following values $3h_e$, $4h_e$ and $5h_e$. The obtained results are compared with the values given by the SED approach. All results are summarized in Figs. 9-14.

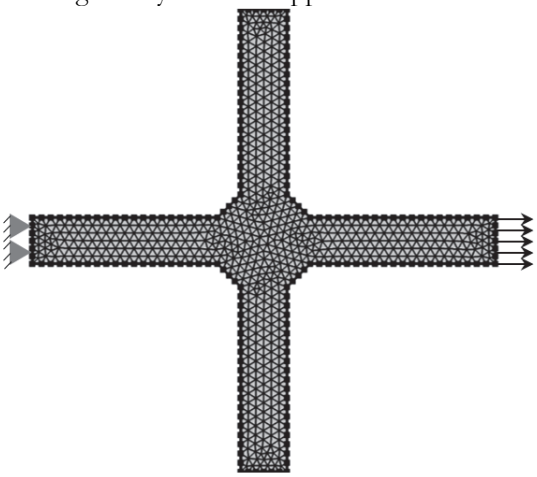

Figure 8: Mesh distribution and boundary condition.

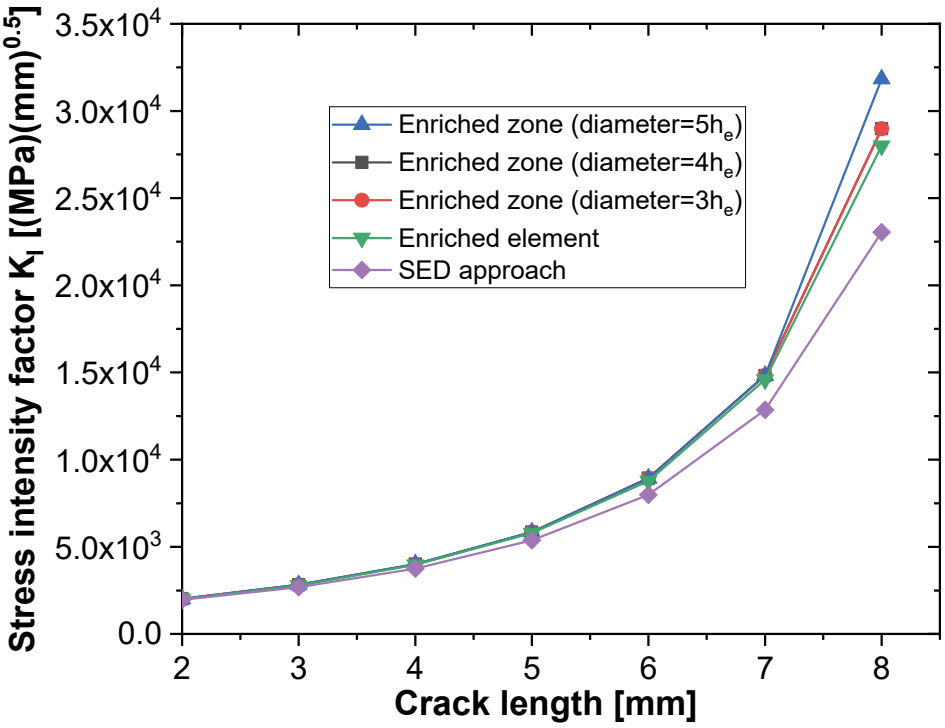

Figure 9: Crack length versus SIF calculated by SED and J-integral with different enriched zone sizes K_I.

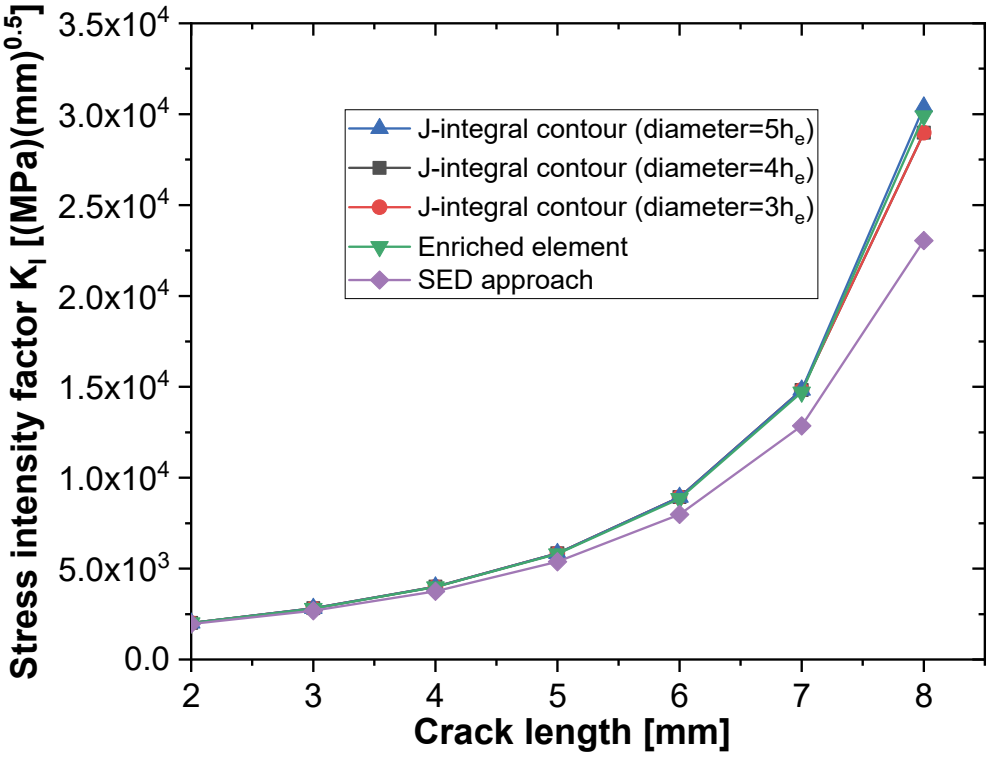

Figure 10: Crack length versus SIF calculated by SED and J-integral with different contour sizes K_I .

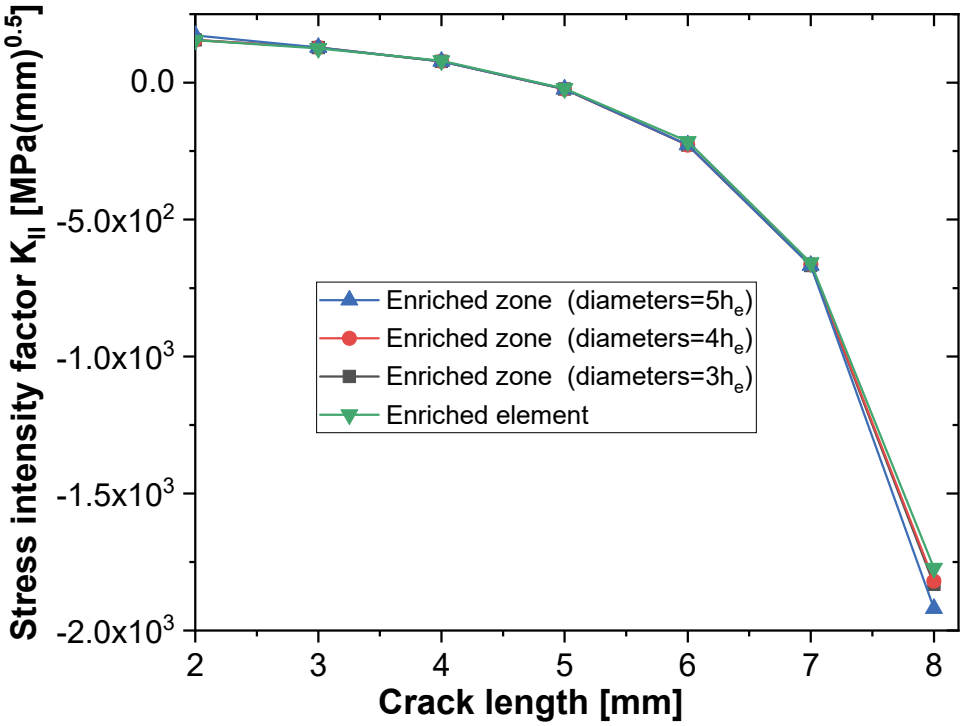

Figure 11: Crack length versus SIF calculated by SED and J-integral with different enriched zone sizes K_{II} .

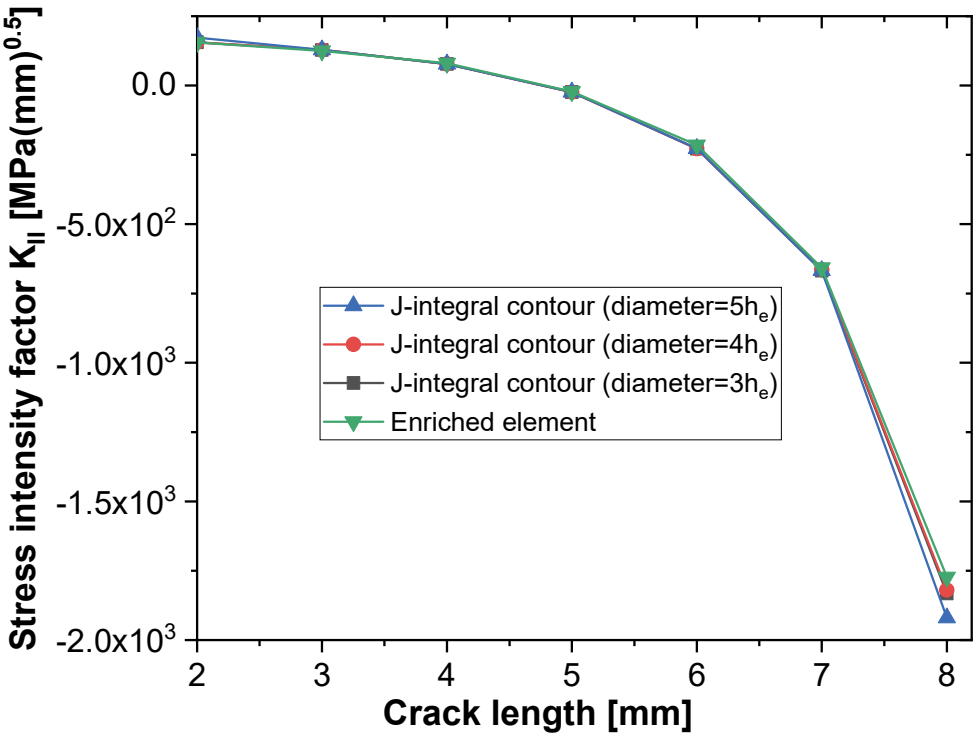

Figure 12: Crack length versus SIF calculated by J-integral with different contour sizes K_{II}.

b) Variation in crack orientation

The same as the previous example by changing the location of the crack angle $\theta = 10, 20, 30, 40, 50, 60, 70, 80, 90$ Fig. 13 to simulate the possibility of defect to the weld root. Changing the contour of the J-Integral was dispensed because there was no effect on the results K_I / K_{II}.

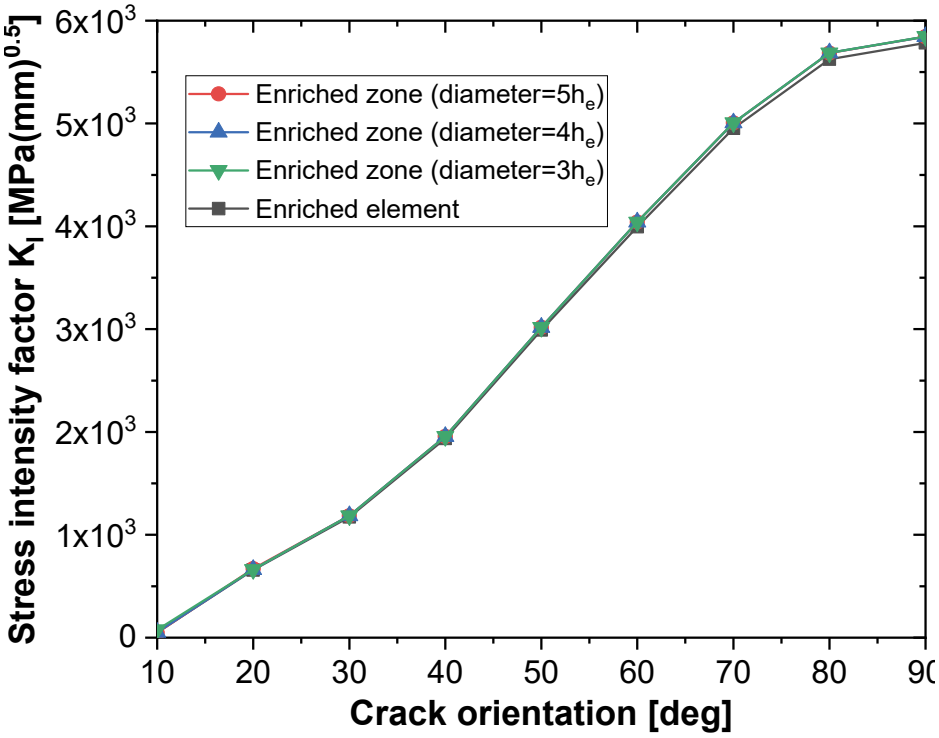

Figure 13: Crack orientation versus SIF calculated J-integral with different enriched zone sizes K_I.

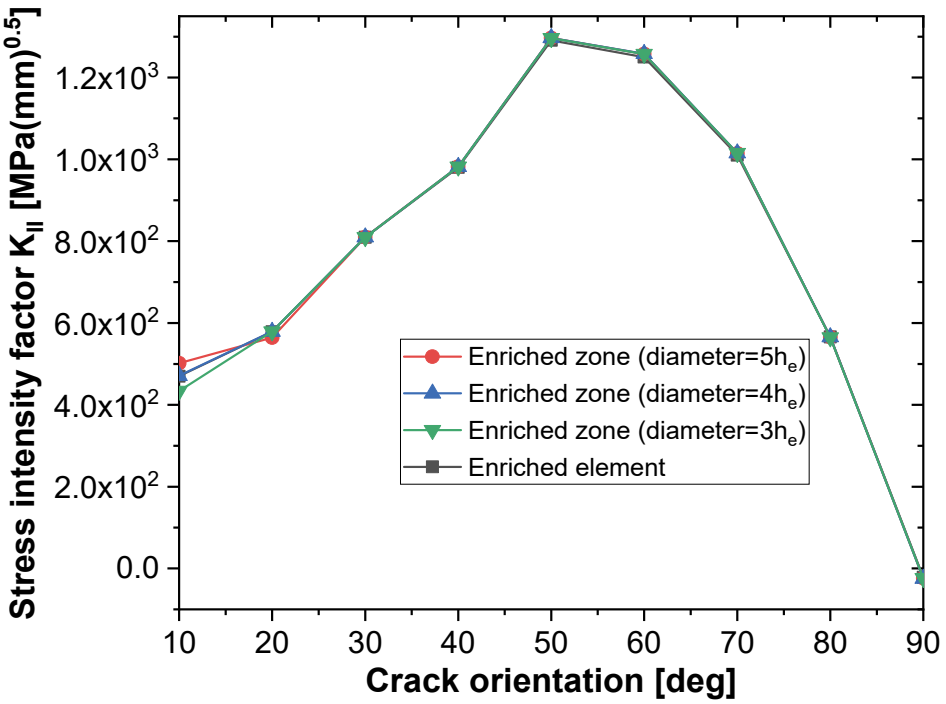

Figure 14: Crack orientation versus SIF calculated J-integral with different enriched zone sizes K_{II} .

Simulation of fatigue crack initiation and propagation

a) Crack initiation

Perform crack initiation and propagation simulation was carried out by XFEM under cyclic loading (all the dimensions, boundary conditions and mesh distribution like the previous example). $\sigma_{max} = 10^6\ Pa$ .Fig. 15 represents the loading changes depending on time. When the crack grows the level set defined by Eqn. (2) is used to make control volume and trace the crack tip and extract the SED value every cycle, through the Eqn. (4) is calculated can calculate SIF value represented in the Fig. 16. After applying load, the element with the maximum principal stress is checked, if the value is greater than ultimate tensile stress these elements contain crack and is oriented towards in the direction of second principal vector and its length at the beginning $2h_e$.

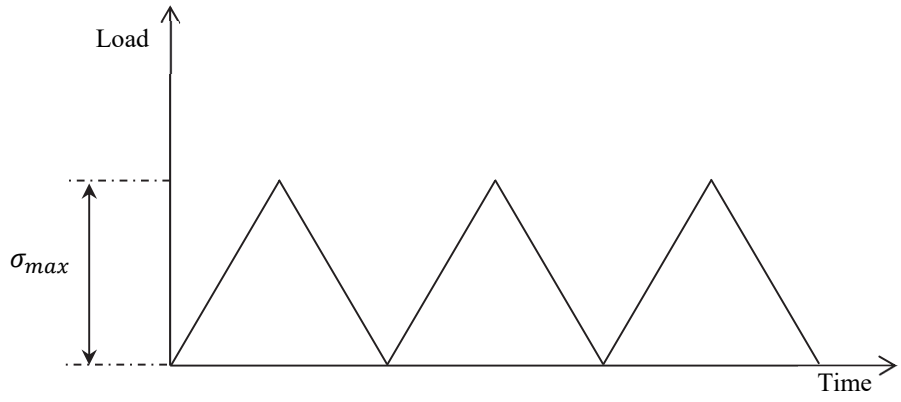

Figure 15: Change the load in terms of time.

b) Crack propagation with different orientation of crack

Perform predefined crack simulation with different orientations $\theta = 60°,70°,80°,90°$ see Fig. 17 was carried out by XFEM under cyclic loading (all the dimensions, boundary conditions, and mesh distribution like the previous example). The results obtained are shown in Fig. 18.

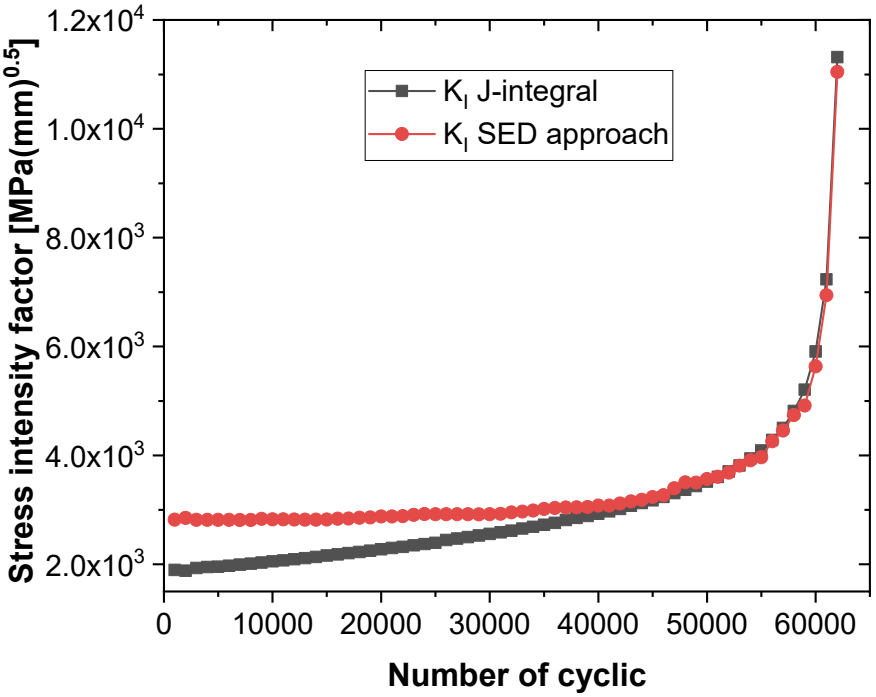

Figure 16: Stress intensity factor K_I versus number of cyclic.

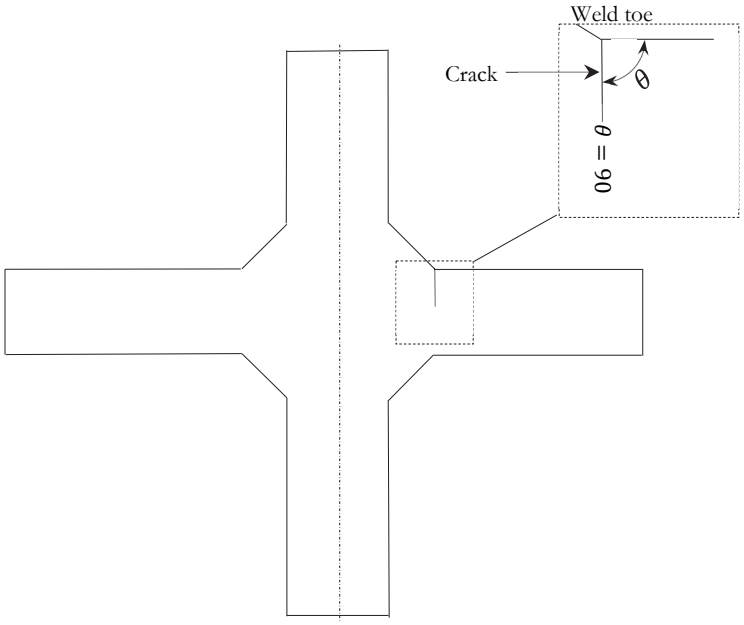

Figure 17: Cruciform welded joints with different crack orientation.

CONCLUSIONS

The fatigue performance of cruciform welded joints made Hardox 450 steel has been studied in this paper, the comparison between the SIF by SED and SIF by J-integral was carried out. The following conclusions can be proposed based on the results:

- The SED approach was used to successfully calculate the mode I, SIF of crack-containing cruciform welded joints using XFEM.

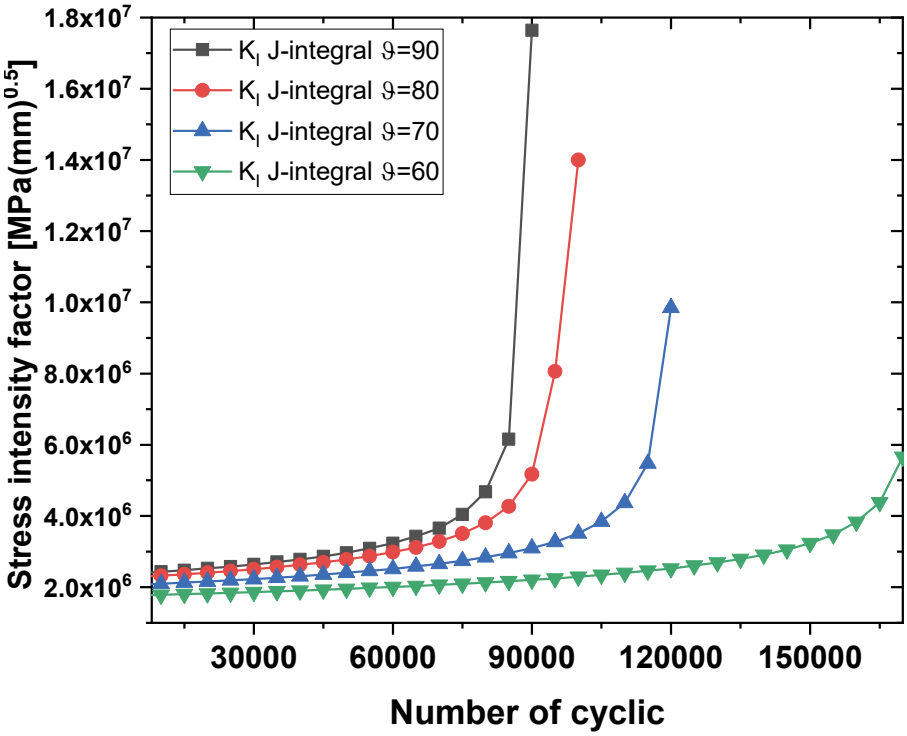

Figure 18: Stress intensity factor K_I versus number of cyclic with different orientation.

- When using XFEM, the SED approach ensures a rapid and simple assessment of the SIF in the case of the cracked component in mode I.
- Has been utilized the level set formulation is used to model the crack and update the crack tip at each cyclic also the control volume is an LST in the form of a circle whose center is a crack tip.
- Despite the complexity of programming the J-integration method, it is the most widely used and stable method for calculating the SIF of cracked components.
- $5h_e$ is considered the radius of the optimal enriched zone.
- The use of XFEM ensures that W_e and SIF values are accurately extracted without a refine mesh.
- In the cruciform welded joints the crack initiation in the weld toe is caused by stress concentration and vicinity to the heat affected area.

REFERENCES

[1] Huang, J.L., Warnken, N., Gebelin, J.C., Strangwood, M., Reed, R.C. (2012). On the mechanism of porosity formation during welding of titanium alloys, Acta Mater., 60(6–7), pp. 3215–3225, DOI: 10.1016/j.actamat.2012.02.035.

[2] Hachi, B.E.K., Rechak, S., Haboussi, M., Taghite, M., Maurice, G. (2008). Fatigue growth of embedded elliptical cracks using Paris-type law in a hybrid weight function approach, Comptes Rendus - Mec., 336(4), pp. 390–397, DOI: 10.1016/j.crme.2008.01.008.

[3] Yang, K., Zhang, Y., Zhao, J. (2020). Elastoplastic fracture analysis of the P91 steel welded joint under repair welding thermal shock based on XFEM, Metals (Basel)., 10(10), pp. 1–26, DOI: 10.3390/met10101285.

[4] Chen, D., Li, G., Wang, Y., Xiao, Q. (2019). Research on fatigue crack propagation of a T-joint based on XFEM and TSA, Eng. Fract. Mech., 222, pp. 106707, DOI: 10.1016/j.engfracmech.2019.106707.

[5] Ma, J., Wang, P., Fang, H. (2021). Fatigue life of 7005 aluminum alloy cruciform joint considering welding residual stress, Materials (Basel), 14(5), pp. 1–20, DOI: 10.3390/ma14051253.

[6] Pang, J.H.L., Tsang, K.S., Hoh, H.J. (2016). 3D stress intensity factors for weld toe semi-elliptical surface cracks using XFEM, Mar. Struct., 48, pp. 1–14, DOI: 10.1016/j.marstruc.2016.04.001.

[7] Montassir, S., Yakoubi, K., Moustabchir, H., Elkhalfi, A., Rajak, D.K., Pruncu, C.I. (2020). Analysis of crack behaviour in pipeline system using FAD diagram based on numerical simulation under XFEM, Appl. Sci., 10(17), DOI: 10.3390/app10176129.
[8] Taheri, S., Tran, V., Julan, E., Robert, N. (2015). Fatigue crack growth and arrest under high-cycle thermal loading using XFEM in presence of weld residual stresses, Transactions, 415 (figure 4).
[9] Kraedegh, A., Li, W., Sedmak, A., Grbovic, A., Trišović, N., Mitrović, R., Kirin, S. (2017). Simulation of fatigue crack growth in a2024-t351 T-welded joint, Struct. Integr. Life, pp. 3–6.
[10] Chatziioannou, K., Karamanos, S.A., Huang, Y. (2019). Ultra low-cycle fatigue performance of S420 and S700 steel welded tubular X-joints, Int. J. Fatigue, 129), pp. 105221, DOI: 10.1016/j.ijfatigue.2019.105221.
[11] Jie, Z., Wang, W., Chen, C., Wang, K. (2021). Local approaches and XFEM used to estimate life of CFRP repaired cracked welded joints under fatigue loading, Compos. Struct., 260, pp. 113251, DOI: 10.1016/j.compstruct.2020.113251.
[12] Nikfam, M.R., Zeinoddini, M., Aghebati, F., Arghaei, A.A. (2019). Experimental and XFEM modelling of high cycle fatigue crack growth in steel welded T-joints, Int. J. Mech. Sci., 153–154, pp. 178–193, DOI: 10.1016/j.ijmecsci.2019.01.040.
[13] Džindo, E., Sedmak, S.A., Grbović, A., Milovanović, N., Đođrević, B. (2019). XFEM simulation of fatigue crack growth in a welded joint of a pressure vessel with a reinforcement ring, Arch. Appl. Mech., 89(5), pp. 919–26, DOI: 10.1007/s00419-018-1435-1.
[14] Gairola, S., Jayaganthan, R. (2021). Xfem simulation of tensile and fracture behavior of ultrafine-grained al 6061 alloy, Metals (Basel), 11(11), DOI: 10.3390/met11111761.
[15] Vempati, S.R., Brahma Raju, K., Venkata Subbaiah, K. (2019). Simulation of Ti-6Al-4V cruciform welded joints subjected to fatigue load using XFEM, J. Mech. Eng. Sci., 13(3), pp. 5371–89, Doi: 10.15282/jmes.13.3.2019.11.0437.
[16] Meneghetti, G., Campagnolo, A. (2018). The Peak Stress Method to assess the fatigue strength of welded joints using linear elastic finite element analyses, Procedia Eng., 213(2017), pp. 392–402, DOI: 10.1016/j.proeng.2018.02.039.
[17] Lazzarin, P., Livieri, P. (2001). Notch stress intensity factors and fatigue strength of aluminum and steel welded joints, Int. J. Fatigue, 23(3), pp. 225–32, DOI: 10.1016/S0142-1123(00)00086-4.
[18] Adib, H., Gilgert, J., Pluvinage, G. (2004). Fatigue life duration prediction for welded spots by volumetric method, Int. J. Fatigue, 26(1), pp. 81–94, DOI: 10.1016/S0142-1123(03)00068-9.
[19] Kired, M.R., Hachi, B.E., Hachi, D., Haboussi, M. (2019). Effects of nano-voids and nano-cracks on the elastic properties of a host medium: XFEM modeling with the level-set function and free surface energy, Acta Mech. Sin. Xuebao, 35(4), pp. 799–811, DOI: 10.1007/s10409-019-00843-4.
[20] Hachi, B.E., Benkhechiba, A.E., Kired, M.R., Hachi, D., Haboussi, M. (2020). Some investigations on 3D homogenization of nano-composite/nano-porous materials with surface effect by FEM/XFEM methods combined with Level-Set technique, Comput. Methods Appl. Mech. Eng., 371, pp. 113319, DOI: 10.1016/j.cma.2020.113319.
[21] Nehar, K.C., Hachi, B.E., Cazes, F., Haboussi, M. (2017). Evaluation of stress intensity factors for bi-material interface cracks using displacement jump methods, Acta Mech. Sin. Xuebao, 33(6), pp. 1051–1064, DOI: 10.1007/s10409-017-0711-6.
[22] Sih, G.C. (1991). Mechanics of Fracture Initiation and Propagation, .
[23] Sih, G.C., Chu, R.C. (1986). Characterization of material inhomogeneity by stationary values of strain energy density, Theor. Appl. Fract. Mech., 5(3), pp. 151–61, Doi: 10.1016/0167-8442(86)90002-9.
[24] Sih, G.C. (1991). Mechanics of Fracture Initiation and Propagation, Dordrecht, Springer Netherlands.
[25] Lazzarin, P., Campagnolo, A., Berto, F. (2014). A comparison among some recent energy- and stress-based criteria for the fracture assessment of sharp V-notched components under mode I loading, Theor. Appl. Fract. Mech., 71, pp. 21–30, DOI: 10.1016/j.tafmec.2014.03.001.
[26] Berto, F., Campagnolo, A., Lazzarin, P. (2015). Fatigue strength of severely notched specimens made of Ti-6Al-4V under multiaxial loading, Fatigue Fract. Eng. Mater. Struct., 38(5), pp. 503–517, DOI: 10.1111/ffe.12272.
[27] Lazzarin, P., Berto, F., Ayatollahi, M.R. (2013). Brittle failure of inclined key-hole notches in isostatic graphite under in-plane mixed mode loading, Fatigue Fract. Eng. Mater. Struct., 36(9), pp. 942–955, DOI: 10.1111/ffe.12057.
[28] Ayatollahi, M.R., Berto, F., Lazzarin, P. (2011). Mixed mode brittle fracture of sharp and blunt V-notches in polycrystalline graphite, Carbon N. Y., 49(7), pp. 2465–2474, DOI: 10.1016/j.carbon.2011.02.015.
[29] Berto, F., Lazzarin, P. (2009). A review of the volume-based strain energy density approach applied to V-notches and welded structures, Theor. Appl. Fract. Mech., 52(3), pp. 183–194, DOI: 10.1016/j.tafmec.2009.10.001.
[30] Torabi, A.R., Ayatollahi, M.R., Colussi, M. (2018). Compressive Brittle Fracture Prediction in Blunt V-Notched PMMA Specimens by Means of the Strain Energy Density Approach, Phys. Mesomech., 21(2), pp. 104–109,

DOI: 10.1134/S1029959918020029.
[31] Moussaoui, M., Amroune, S., Tahiri, A., Hachi, B.K. (2020). Brittle fracture investigation from disc specimen weakened by U-notch in mixed mode I + II, Eng. Solid Mech., 8(4), pp. 337–352, DOI: 10.5267/j.esm.2020.3.004.
[32] Lazzarin, P., Zambardi, R. (2002). The equivalent strain energy density approach re-formulated and applied to sharp V-shaped notches under localized and generalized plasticity, Fatigue Fract. Eng. Mater. Struct., 25(10), pp. 917–928, DOI: 10.1046/j.1460-2695.2002.00543.x.
[33] Lazzarin, P., Berto, F., Zappalorto, M. (2010). Rapid calculations of notch stress intensity factors based on averaged strain energy density from coarse meshes: Theoretical bases and applications, Int. J. Fatigue, 32(10), pp. 1559–1567, DOI: 10.1016/j.ijfatigue.2010.02.017.
[34] Aliha, M.R.M., Berto, F., Bahmani, A., Gallo, P. (2017). Mixed mode I/II fracture investigation of Perspex based on the averaged strain energy density criterion, Phys. Mesomech., 20(2), pp. 149–156, DOI: 10.1134/S1029959917020059.
[35] Aliha, M.R.M., Berto, F., Bahmani, A., Akhondi, S., Barnoush, A. (2016). Fracture assessment of polymethyl methacrylate using sharp notched disc bend specimens under mixed mode I + III loading, Phys. Mesomech., 19(4), pp. 355–364, DOI: 10.1134/S1029959916040020.
[36] Campagnolo, A., Berto, F. (2015). Tensile fracture analysis of blunt notched pmma specimens by means of the strain energy density, Eng. Solid Mech., 3(1), pp. 35–42, DOI: 10.5267/j.esm.2014.12.001.
[37] Pook, L.P., Campagnolo, A., Berto, F., Lazzarin, P. (2015). Coupled fracture mode of a cracked plate under anti-plane loading, Eng. Fract. Mech., 134, pp. 391–403, DOI: 10.1016/j.engfracmech.2014.12.021.
[38] Mirsayar, M.M., Berto, F., Aliha, M.R.M., Park, P. (2016). Strain-based criteria for mixed-mode fracture of polycrystalline graphite, Eng. Fract. Mech., 156, pp. 114–123, DOI: 10.1016/j.engfracmech.2016.02.011.
[39] Meneghetti, G., Campagnolo, A., Berto, F. (2015). Some relationships between the peak stresses and the local strain energy density for cracks subjected to mixed-mode (I+II) loading, Frat. Ed Integrita Strutt., 9(33), pp. 33–41, DOI: 10.3221/IGF-ESIS.33.05.
[40] Shin, W.S., Chang, K.H., Muzaffer, S. (2021). Fatigue analysis of cruciform welded joint with weld penetration defects, Eng. Fail. Anal., 120, pp. 105111, DOI: 10.1016/j.engfailanal.2020.105111.
[41] Jie, Z., Berto, F., Susmel, L. (2020). Fatigue behaviour of pitted/cracked high-strength steel wires based on the SED approach, Int. J. Fatigue, 135(October 2019), pp. 105564, DOI: 10.1016/j.ijfatigue.2020.105564.
[42] Lazzarin, P., Lassen, T., Livieri, P. (2003). A notch stress intensity approach applied to fatigue life predictions of welded joints with different local toe geometry, Fatigue Fract. Eng. Mater. Struct., 26(1), pp. 49–58, DOI: 10.1046/j.1460-2695.2003.00586.x.
[43] Fischer, C., Fricke, W., Rizzo, C.M. (2016). Experiences and recommendations for numerical analyses of notch stress intensity factor and averaged strain energy density, Eng. Fract. Mech., 165, pp. 98–113, DOI: 10.1016/j.engfracmech.2016.08.012.
[44] Gaiotti, M., Rizzo, C.M., Berto, F. (2017). Assessment of Welded Joints by Strain Energy Density Approach Accounting for Misalignments and Geometrical Imperfections. Materials Technology, American Society of Mechanical Engineers, 4, pp. 1–7.
[45] Braun, M., Fischer, C., Fricke, W., Ehlers, S. (2020). Extension of the strain energy density method for fatigue assessment of welded joints to sub-zero temperatures, Fatigue Fract. Eng. Mater. Struct., 43(12), pp. 2867–2882, DOI: 10.1111/ffe.13308.
[46] Lazzarin, P., Zambardi, R. (2001). A finite-volume-energy based approach to predict the static and fatigue behavior of components with sharp V-shaped notches, Int. J. Fract., 112(3), pp. 275–298, DOI: 10.1023/A:1013595930617.
[47] Fries, T.-P., Belytschko, T. (2010). The extended/generalized finite element method: An overview of the method and its applications, Int. J. Numer. Methods Eng., 84(3), pp. 253–304, DOI: 10.1002/nme.2914.
[48] Zi, G., Belytschko, T. (2003). New crack-tip elements for XFEM and applications to cohesive cracks, Int. J. Numer. Methods Eng., 57(15), pp. 2221–2240, DOI: 10.1002/nme.849.
[49] Moës, N., Belytschko, T. (2002). X-FEM, de nouvelles frontières pour les éléments finis, Rev. Eur. Des Éléments Finis, 11(2–4), pp. 305–18, DOI: 10.3166/reef.11.305-318.
[50] Menouillard, T., Belytschko, T. (2010). Dynamic fracture with meshfree enriched XFEM, Acta Mech., 213(1–2), pp. 53–69, DOI: 10.1007/s00707-009-0275-z.
[51] Paris, P., Erdogan, F. (1963). A critical analysis of crack propagation laws, J. Fluids Eng. Trans. ASME, 85(4), pp. 528–33, DOI: 10.1115/1.3656900.
[52] Tanaka, K. (1974). Fatigue crack propagation from a crack inclined to the cyclic tensile axis, Eng. Fract. Mech., 6(3), DOI: 10.1016/0013-7944(74)90007-1.
[53] Kumar, S., Wang, Y., Poh, L.H., Chen, B. (2018). Floating node method with domain-based interaction integral for

generic 2D crack growths, Theor. Appl. Fract. Mech., 96(November), pp. 483–496, DOI: 10.1016/j.tafmec.2018.06.013.
[54] Stolarska, M., Chopp, D.L. (2003). Modeling thermal fatigue cracking in integrated circuits by level sets and the extended finite element method, Int. J. Eng. Sci., 41(20), pp. 2381–410, DOI: 10.1016/S0020-7225(03)00217-9.
[55] Pais, M.J., Kim, N. (2009). Finite Element and Level Set Methods, Aerospace, pp. 1–16.
[56] Morre, M.A. (1975). The abrasive wear resistance of surface coatings, J. Agric. Eng. Res., 20(2), pp. 167–179, DOI: 10.1016/0021-8634(75)90084-0.
[57] Konat, Ł., Zemlik, M., Jasiński, R., Grygier, D. (2021). Austenite grain growth analysis in a welded joint of high-strength martensitic abrasion-resistant steel hardox 450, Materials (Basel), 14(11), DOI: 10.3390/ma14112850.
[58] Reitz, W. (2006). A Review of: Welding Metallurgy and Weldability of Stainless Steel, Mater. Manuf. Process, pp. 219–219, DOI: 10.1080/10426910500476747.
[59] Treifi, M., Oyadiji, S.O. (2013). Strain energy approach to compute stress intensity factors for isotropic homogeneous and bi-material V-notches, Int. J. Solids Struct., 50(14–15), pp. 2196–2212, DOI: 10.1016/j.ijsolstr.2013.03.011.
[60] Berto, F., Razavi, S.M.J., Ayatollahi, M.R. (2017). Some methods for rapid evaluation of the mixed mode NSIFs, Procedia Struct. Integr., 3, pp. 126–134, DOI: 10.1016/j.prostr.2017.04.022.
[61] Treifi, M., Oyadiji, S.O. (2013). Evaluation of mode III stress intensity factors for bi-material notched bodies using the fractal-like finite element method, Comput. Struct., 129, pp. 99–110, DOI: 10.1016/j.compstruc.2013.02.015.
[62] Pittarello, L., Campagnolo, A., Berto, F. (2016). NSIFs estimation based on the averaged strain energy density under in-plane mixed mode loading, Procedia Struct. Integr., 2, pp. 1829–1836, DOI: 10.1016/j.prostr.2016.06.230.
[63] Song, W., Liu, X., Berto, F., Wang, P., Fang, H. (2017). Fatigue failure transition analysis in load-carrying cruciform welded joints based on strain energy density approach, Fatigue Fract. Eng. Mater. Struct., 40(7), pp. 1164–1177, DOI: 10.1111/ffe.12588.
[64] Song, W., Liu, X., Razavi, S.M.J. (2018). Fatigue assessment of steel load-carrying cruciform welded joints by means of local approaches, Fatigue Fract. Eng. Mater. Struct., 41(12), pp. 2598–2613, DOI: 10.1111/ffe.12870.